Design Considerations for an UWB Computationally-Efficient Fast Acquisition System for Indoor Line-of-Sight Ranging Applications

Yassine Salih-Alj, *Member, IEEE,* Charles Despins, *Senior Member, IEEE,* and Sofiène Affes, *Senior Member, IEEE*

***Abstract*—This paper presents an Ultra-Wideband (UWB) computationally-efficient fast acquisition system suggested for ranging in indoor, Line-Of-Sight (LOS) environments. The performance of the proposed scheme is evaluated and its implementation issues are discussed. The design complexity leverages field-programmable gate arrays (FPGA) to implement the parallel processing concept. Timing acquisition at high sampling rates of the ultra-short pulses used in UWB communications can be costly and slow for ranging. This is due to the large number of required operations in an intensive software-based signal processing. The proposed UWB scheme in this paper uses an efficient block-processing technique that simplifies hardware implementation with a greatly reduced number of operations and acquisition time, while also offering accurate ranging capabilities over the considered indoor channel at high levels of multiple-user interference (MUI) and Gaussian noise.**

***Index Terms*—Ranging, pulse shape, acquisition, ultra-wideband.**

I. Introduction

ULTRA-WIDEBAND (UWB) technology is currently regarded as an attractive solution for many wireless applications where high resolution, reduced interference, and propagation around obstacles are challenging [1], [2]. It utilizes ultra-short pulse shapes transmitted at a very low Power Spectral Density (PSD) in compliance to the Federal Communications Commission (FCC) rules that defined UWB signals with a fractional bandwidth greater than or equal to 0.2 of the center frequency or a bandwidth of at least 500 MHz [3].

Timing acquisition is known as one of the key technical aspects that influence the successful development of UWB systems. In fact, the extremely narrow time frames and implicitly the required high sampling rates make signal acquisition and the overall UWB transceiver design/operation a challenging task from a technical viewpoint [5]. In recent years, much research work has been devoted to accelerating the acquisition process of UWB signals. Based on different algorithmic approaches, several fast acquisition techniques were proposed [6]-[11]. However, the complexity aspect was generally less emphasized than the algorithmic one. Indeed, the correlations are computed in the time domain and acquisition systems are fed by stream processing, sample by sample, irrespective of the search strategy (serial or parallel) [5]. The corresponding architectures are thus not optimal and may require relatively long processing times under challenging conditions, e.g., inside an underground mine gallery, a peculiar, harsh and infrequently studied environment [12], [13] where Line-Of-Sight (LOS) ranging applications are highly desirable for safety and efficiency purposes. However, UWB technology, as a physical support with excellent temporal resolution, is very promising for such applications [14]. In order to achieve a low-complexity receiver, an UWB computationally-efficient acquisition system showing explicit design characteristics that offer greatly improved computational cost and acquisition time was proposed in [15].

In this paper, we evaluate the performance of this new UWB fast acquisition system suggested for ranging over this peculiar multipath fading channel. The suggested scheme, based on a block-processing technique adapted to a high-speed frequency correlator by a cubic spline interpolation, is validated by performance comparisons under different scenarios of interference and Gaussian noise. Furthermore, in addition to the PSD of the transmitted signal which is influenced by the used pulse shape, the performance of the UWB system itself may also be affected under non-ideal conditions [16]. Thus, the choice of the fundamental pulse shape to adopt within the system is one of the most important considerations that may affect its performance. In [17], the first ten Gaussian derivatives were compared in terms of their PSD and compliance to the FCC spectral constraints. For these pulses, higher-order derivatives have shown a better fit to the FCC masks with a decreasing bandwidth as the order of the derivative increases. Moreover, Gaussian-based pulse shapes outperform generally other UWB typical pulse types, as recently proposed in [18], and are noticeably easier to generate [19]. These observations lead to considering Gaussian-based waveforms, typically high-order derivatives, as the most potential candidates for the suggested UWB system.

The remainder of this paper is organized as follows. In Section II, the system model is given. Section III details the proposed UWB fast acquisition system with its implementation issues, followed by Section IV that provides simulation results, and finally Section V concludes the paper.

Manuscript received December 2, 2010; revised March 8, 2011; accepted April 28, 2011. The associate editor coordinating the review of this manuscript and approving it for publication was S. Ghassemzadeh.

This work was supported by Bell Nordic Group, Inc. and was presented in part at IEEE ICC'08, Beijing, China, May 2008.

Y. Salih-Alj is with the School of Science & Engineering, Al Akhawayn University in Ifrane, Morocco (e-mail: Y.SalihAlj@aui.ma).

C. Despins is withPrompt, Inc. Canada (e-mail: cdespins@promptinc.org).

S. Affes is with INRS-EMT, Montreal, Canada (e-mail: affes@emt.inrs.ca).

Digital Object Identifier 10.1109/TWC.2011.060811.102158

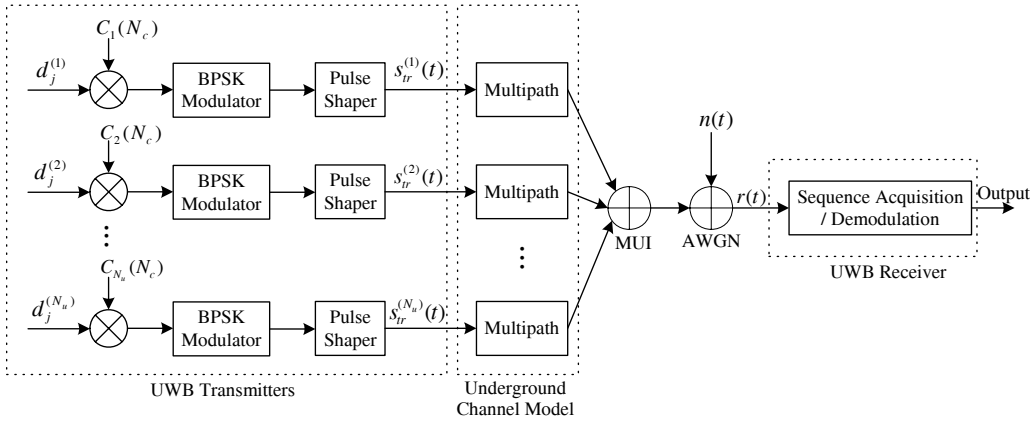

Fig. 1. Block diagram of the considered system model.

II. System Model

In this section, we will describe the system model of the considered UWB communication system.

A. UWB Transmitter

The Direct-Sequence (DS) UWB concept is employed in this paper with BPSK (Binary Phase Shift Keying) pulse signaling. The pulse occupies the entire chip interval and is transmitted continuously according to a MLS (Maximum Length Sequence) spreading code. The DS-UWB signal transmitted by a user k can typically be expressed as

$$s_{tr}^{k}(t) = \sum_{j=-\infty}^{+\infty} \sum_{n=0}^{N_c-1} d_j^{(k)} c_n^{(k)} p_{tr}(t - jT_f - nT_c), \quad (1)$$

where $p_{tr}(t)$ represents the transmitted pulse shape (i.e., Gaussian 3^{rd}-order derivative), $\{dj\}$ represent the modulated data symbols mapped into $\{-1, 1\}$, $\{c_n\}$ are the spreading chips generated according to a MLS code, T_c is the chip duration. There are N_c chips per each message symbol j of period T_f − the spreading factor − such that $N_c.T_c = T_f$.

B. Pulse Shape

The transmitted pulse shape used within an UWB system influences its spectral properties. The considered ultra-short pulse duration Tc is 2 ns. So the effective UWB signal bandwidth is at least 500 MHz. Moreover, due to antenna effects, the processed pulse at the receiver is modeled as a derivative of the transmitted pulse shape. The basic Gaussian pulse is expressed as

$$p(t) = \frac{1}{\sqrt{2\pi}\sigma} \exp\left(-\frac{t^2}{2\sigma^2}\right), \quad (2)$$

where σ is a shape factor used typically as a bandwidth decaying parameter. The n^{th}-order Gaussian derivative can be determined recursively from

$$p_n(t) = -\frac{n-1}{\sigma^2} p_{n-2}(t) - \frac{t}{\sigma^2} p_{n-1}(t). \quad (3)$$

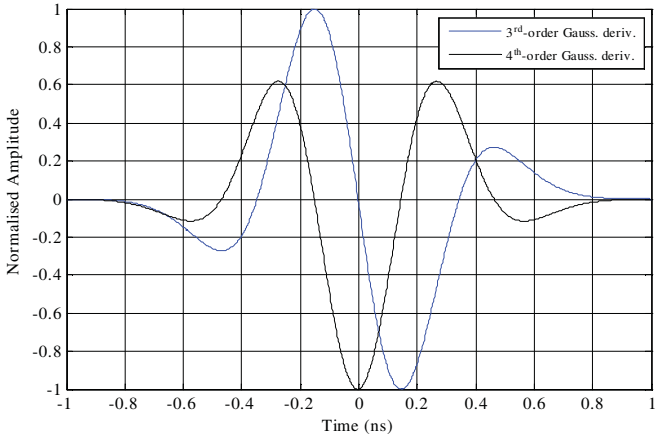

Fig. 2. 3^{rd} and 4^{th}-order Gaussian derivatives pulse shapes in time domain.

The amplitude spectrum of the n^{th}-order Gaussian derivative, obtained from its Fourier transform, is

$$|X_n(f)| = (2\pi f)^n \exp\left(-\frac{(2\pi f\sigma)^2}{2}\right). \quad (4)$$

By differentiating (4) and setting it equal to zero, the peak transmission frequency f_p, at which the maximum is attained, can be found to satisfy the following:

$$2\pi f_p \sigma = \sqrt{n}. \quad (5)$$

Then, the Gaussian derivatives of higher orders are characterized by a higher peak frequency while reducing the shape factor σ shortens the pulse. Notice that for a maximized PSD the first order Gaussian derivative does not meet the FCC spectral requirement no matter what pulse width value is used. In fact, the pulse shape must efficiently fill the FCC spectrum mask for maximum allowable transmit power [17], [20]. Additionally, to make the pulse spectrum meet the masks for a maximized PSD, compressing the spectrum by adjusting the scaling factor could not be done because changing the scaling factor also changes the center frequency in such a way that the spectrum fail to meet the mask [18]. Hence, increasing the order of the derivative results in a wider overall pulse width for each successive pulse and, consequently, in a narrower bandwidth around the same center frequency, thereby

showing a better fit to the FCC masks. Indeed, as the pulse order increases, the number of zero crossings in the same pulse width also increases. The pulses then begin to resemble sinusoids modulated by a Gaussian pulse-shaped envelope, thus corresponding to a higher "carrier" frequency sinusoid modulated by an equivalent Gaussian envelope [16].

C. UWB Channel Model

The considered discrete impulse response of the UWB channel model used herein is expressed as follows:

$$h(t) = \sum_{l=0}^{L-1} \alpha_l \delta(t - \psi_l), \tag{6}$$

where $\delta(t)$ is the Dirac delta function, L is the number of multipath components; α_l and ψ_l are, respectively, the gain and the delay introduced by the l^{th} path of the channel. Note that a complex tap model is not adopted here. The complex baseband model is a natural fit for narrowband systems to capture the channel behavior independently of the carrier frequency. But it has clear limitations for UWB systems where a real-valued model at RF is more natural [21]. As for the IEEE.802.15.3a standard model, a log-normal distribution has been used for the multipath gain. For the data measurements obtained in a mining environment, this distribution was confirmed by the Kolmogorov-Smirnov test [22] from data measurements obtained in an underground mine, the environment which we consider in this paper for an indoor LOS ranging application.

Furthermore, as in the Saleh-Valenzuela model [23], the first ray starts by definition at $t = 0$, and the successive rays arrive with a rate given by a Poisson process with rate $\lambda = 1.15\ (\text{ns})^{-1}$ (i.e., of 2.3 rays per chip). The power of these rays decays exponentially with increasing delay from the first ray. However, for the considered mining environment, and in contrast to what was reported for more conventional indoor environments with smooth surfaces [21], [23], [24], no path clustering effect was observed, neither in NB/WB (Narrow-Band/Wide-Band) measurements [13], nor in the LOS scenario as disclosed in a recent UWB measurement work carried out in such confined environments with rough surfaces [22]. Indeed, a LOS scenario can be assumed for indoor ranging applications [25]. Since this work is intended for a ranging application in an underground mine environment as a possible application, we focus only on the LOS scenario where the first path is assumed to be the direct and the strongest from which the time of flight (TOF) is relatively estimated. In such a peculiar confined environment, the LOS scenario can be assumed with an appropriate physical distribution of the static nodes within the considered mine gallery. So the mobile receiver node would continuously have a direct LOS with a least three static transmitters.

Figs. 3 and 4 show, respectively, a typical underground impulse response and its corresponding log-normal PDF. A threshold of 40 dB below the strongest path was chosen to avoid the effect of noise on the statistics of multipath channel [22]. Hence for the sake of simplicity, we consider the impulse response restricted to $L = 3$ paths (i.e., two interfering paths to the direct first path). As for our ranging application, we focus on the direct path (i.e., strongest), with a gain normalized to unity in the simulations. The log-normal fading statistics of the two interfering paths are as expressed in Table I. Their relative variance is, as it seems intuitively clear, smaller for small gains than for large ones, a fact that was confirmed, e.g., in [26]. Indeed, among the few available studies related to underground mine impulse response structure, three dominant propagation paths were typically observed with the first path as the strongest [27], [13], [28], [29].

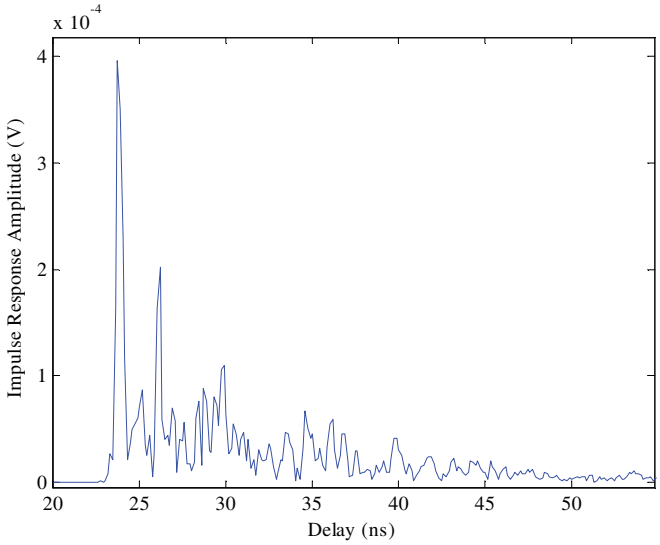

Fig. 3. Typical underground impulse response in LOS obtained by channel sounding.

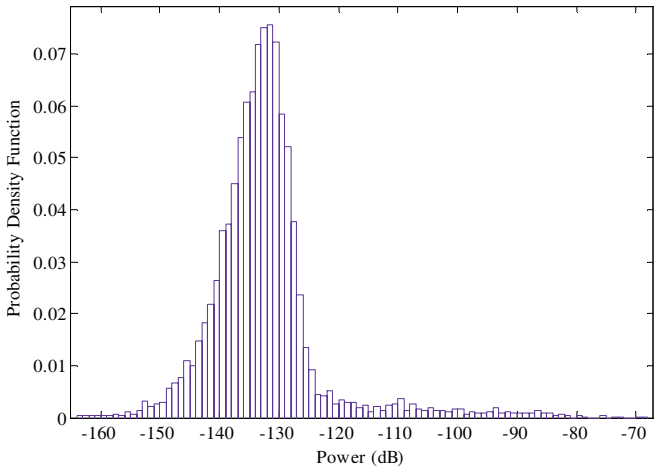

Fig. 4. Probability Density Function of the received signal in LOS scenario.

TABLE I
LOGNORMAL FADING PARAMETERS

Interfering Paths	Lognormal Statitics	
	E[α_l]	Var[α_l]
$l = 1$	0.5	0.09
$l = 2$	0.25	0.04

D. UWB Receiver

When Nu users are active within the system, while focusing on the transmitter k, the signal at the receiver can be modeled as

$$r(t) = \sum_{l=0}^{2} \alpha_l^{(k)} s_{pr}^{(k)}(t - \theta_l^{(k)}) + n_g(t), \tag{7}$$

where α_l is the amplitude fading factor on the l^{th} path, θ_l is a summation of the delay ψ_l exclusively introduced by the l^{th} path and the phase-shift $\tau^{(k)}$ that corresponds to the TOF between the transmitter k and the considered receiver. θ_l is exponentially distributed such as

$$\mu_{exp} = \frac{1}{\lambda} = 0.87, \tag{8}$$

and $n_g(t)$ is expressed as

$$n_g(t) = \sum_{\substack{q=l \\ q \neq k}}^{N_u} \sum_{l=0}^{2} \alpha_l^{(q)} s_{pr}^{(q)}(t - \theta_l^{(q)}) + n(t), \tag{9}$$

in which $s_{pr}(t)$ corresponds to $p_{pr}(t)$, the processed pulse shape at the receiver (antenna effect). $n(t)$ represents the received Gaussian noise modeled as $N(0, \sigma_n^2)$ with a power spectral density of σ_n^2. Furthermore, as the signals are transmitted over an underground mine environment, the system model illustrated in Fig. 1 considers interference coming only from the UWB users. Indeed, the considered UWB wireless technology is assumed a worthy candidate to replace narrowband signals in such confined area. Thus, the considered system model in this paper focuses only on UWB interferers.

Moreover, the fading factor α_l of the interfering paths is log-normally distributed, as characterized by [30]

$$\mu_{Nrm} = \ln(m_1) = -\frac{1}{2} \ln\left(\frac{m_2}{m_1^2}\right), \tag{10}$$

and

$$\sigma_{Nrm}^2 = \ln\left(\frac{m_2}{m_1^2}\right), \tag{11}$$

where m_1 and m_2 are the two first empirical moments corresponding to the values expressed in Table I (knowing that m_1 =E[α_l] and m_2 =Var[α_l] + m_1^2). Accordingly, the distribution parameters of the fading factor α_l are deduced as

$$20 \log_{10}(\alpha_l) \propto \mathrm{N}(-0.8469, 0.3075), \tag{12}$$

and

$$20 \log_{10}(\alpha_2) \propto \mathrm{N}(-1.6336, 0.4947). \tag{13}$$

Finally, note that this synthesized UWB channel model is used in this paper as a physical support for the considered underground mining environment. Furthermore, as ranging is a prerequisite step in any positioning application, positioning in such a challenging indoor LOS environment is mentioned as a potential application for the suggested UWB fast acquisition scheme that can be nonetheless generically used for different environments.

III. DS-UWB Fast Acquisition System

A. Processing Technique

The *Block-Processing* technique was used with an *FFT-based* (Fast Fourier Transform) *high-speed* frequency correlator that offered a fast and accurate acquisition of the dense DS-UWB signal with optimal receiver complexity. This method suggested for UWB signal acquisition is valuable in view of its efficiency in real time handling of high data throughputs [31] and has shown high effectiveness in other fields [32]-[35]. The acquisition process is accelerated by handling the dense UWB signal in simultaneous blocks of samples and by reducing efficiently the computational cost.

The samples of the acquired UWB signal are stored in blocks as they arrive. The processing of a block starts when its last sample arrives and proceeds simultaneously with the storage of the next block. Block-Processing techniques can be used when the input sample rate is much greater than the output sample rate [31]. For a DS-UWB receiver, processing is performed on each acquired block i to evaluate a code phase-shift τ_i and a Signal to Interference plus Noise Ratio $SINR_i$. Since the block must cover at least a whole spreading code period (i.e., several hundred samples), and the output is only two values per block, the conditions for block processing are satisfied.

Synchronization is performed by an FFT-based circular correlator fed by the handled blocks. The block length M is taken as of power-of-two; thus the used FFTs have an optimal butterfly structure. Hence, the correlation is computed in the frequency domain by a simple multiplication, producing the same result as the standard correlation but faster with this high-speed correlation technique. The fast correlator structure can be further optimized by avoiding the FFT used for the local replica which can be pre-calculated. Therefore, the correlator will require only one FFT/IFFT pair. The processed DS-UWB received signal can be modeled as

$$r_{i,u}^{(j,N_u)} = d_{u,\tau_i}^{(j,k)} c_{i,\tau_i}^{(j,k)} p_{pr}\left((m_i + u) - jT_f - \frac{N_c}{M}(m_i + u)T_c - \tau_i^{(k)}\right) + n_{f_{(i,u)}}^{(k)} + n_{g_{(i,u)}}^{N_u}, \tag{14}$$

where $p_{pr}()$ represents the processed pulse shape at the receiver (antenna derivative effect), $n_f^{(k)}$ is the interference signal resulting from the interfering paths with respect to the acquired user's signal, u refers to the u^{th} sample ($u = 1, 2, ..., M$) of the i^{th} block, m_i is the total number of samples before the i^{th} block ($m_i = (i-1) \cdot M$) and k corresponds to the acquired user at the receiver. Since the considered UWB communication system is only used for ranging purposes, the data symbols $\{d\}$ are set to 1.

The received signal $\{r_{i,u}\}$ and the local pulse-shaped replica corresponding to the acquired MLS spreading code $\{c_{i,\tau_i}\}$ are both finite length sequences being handled in blocks; hence, their correlation can be carried out by a slight modification of the circular convolution operation. Indeed, the correlation of these two sequences is obtained by considering the product of their discrete Fourier transforms DFTs while the local pulse-shaped replica is time reversed, thus a complex

conjugate is applied. Therefore, the resulting correlation performed in the frequency domain, $\{R_{i,u}\}$, of the i^{th} received signal block, $\{r_{i,u}\}$, with the local pulse-shaped replica of the k^{th} user, can be expressed as follows:

$$R_{i,u}^{(k)} = \text{IDFT}\left\{\text{DFT}\left\{r_{i,u}^{(N_u)}\right\} \cdot \text{DFT}^* \left\{c_i^{(k)} p_{pr}\left[(m_i+u)\cdot\left(1-\tfrac{N_c T_c}{M}\right)\right]\right\}\right\}. \quad (15)$$

In practice, the FFT is used as an efficient algorithm to calculate the DFTs required in this frequency-domain correlation operation.

B. UWB Acquisition Scheme

The block diagram of the proposed UWB fast acquisition system is shown in Fig. 5. Its significant parameters include: a spreading factor $N_c = 63$; a pulse duration $T_p = T_c = 2$ ns (a duty cycle of 100 %); number of samples per chip $N_s = 16$ (sampling frequency $F_s = N_s/T_c = 8$ GHz); a Gaussian 4^{th}-order derivative as the acquired pulse waveform; and an increased block length $M = (1 + N_c) \cdot N_s = 1024$. Notice that recent developments in research institutions and industry promise high sampling rates with great resolutions for both ADCs (Analog-to-Digital Converter) and FFTs [36], [37].

An *over-sampling* method is required for adapting as efficiently as possible the acquired block's length to the FFTs with a butterfly structure. Thus, the cardinality of the blocks digitized by the ADC converter should be increased from 1008 samples to 1024 (a power-of-two). Then the correlation is calculated in the frequency domain by a fast circular correlator. A peak detector examines its outputs (1024 inverse-FFT outputs) to evaluate the detected peak amplitude and to infer its position which corresponds to the estimated phase-shift τ_i. Note that the resulting peaks within the acquired UWB blocks are spaced far enough to make their separation apart possible with a simple peak detector; thereby allowing a fast processing of such dense signal. During the acquisition process, the peak detector simultaneously searches the maximum amplitude through the 1024 incoming values from the correlator, and the corresponding peak's position is determined (using a counter which counts from 0 to 1023). Therefore, for each acquired block i, the estimated phase-shift in samples can be computed as follows:

$$\tau_i = \left(\frac{\tau_{i(1024)}}{1024} \times 1008\right) (\text{samples}), \quad (16)$$

where τ_i is the estimated phase-shift in samples and $\tau_{i(1024)}$ is the peak position within a block of 1024 samples. The more blocks are acquired, the more refined will be that estimated phase which represents the TOF required for ranging with respect to the acquired user k. To locate itself, the claimant (i.e., receiver) can use 2D-trilateration with respect to two *verifiers* (i.e., static transmitters). If no peak is detected according to a detection threshold D_T, the search control block leads the local code generator index to the next pre-calculated replica $k+1$. Furthermore, in order to characterize the relative amplitude of the detected peak with respect to false correlations due to interferences and noise, an acquisition margin is considered above D_T. Since the direct path energy is normalized to unity, an acquisition margin of 14.9 dB can be used for the detection if the noise level is set as low as 18 %.

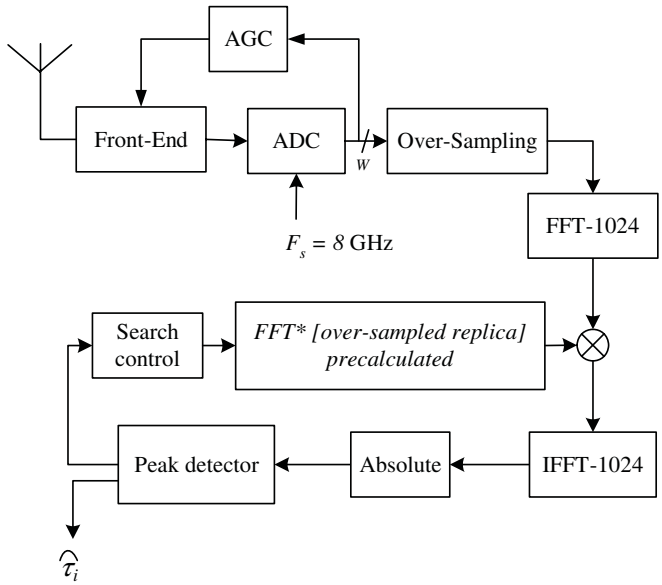

Fig. 5. Block diagram of the proposed UWB fast acquisition system.

C. Implementation Issues

The proposed fast acquisition system promises efficient handling of the dense UWB signal. However, in the prospect of a practical implementation of such a high-data rate scheme, the related design complexity is analyzed with respect to current VLSI (Very-Large-Scale Integration) chips for a given quantization level. Recently, some research work focused on the quantization resolution used by the ADC to sample the nanosecond impulses into Giga Samples Per Second (GSPS) range, to capture faithfully the carried information. Fortunately, the used BPSK modulation scheme does not need a high resolution ADC. According to [38], a 4-bit resolution is sufficient for impulse UWB. In [39], an UWB rake receiver was proposed with a single-bit sampling quantization. It offered significantly reduced complexity and power consumption, at the price of a SNR degradation limited to 2 dB in comparison to a conventional receiver based on a CMOS 4-bit ADC operating at 12 GSPS [40]. Lately in [41], a low-power consumption ADC was proposed for UWB signals with a sampling resolution of 4 bits. Note that for such quantization over one bit, an automatic gain control (AGC) is necessary for optimally using the ADC dynamic range. A 4-bit quantization (i.e., $W = 4$ bits in reference to Fig. 5) is adopted, hence using 16 amplitude levels in abscissa (i.e., $2^{4\,\text{bits}}$) for the 16 samples in ordinate (i.e., 8 GSPS $\cdot$ 2 ns), thus 15 threshold comparators are required. Note that a 0.11 μm CMOS comparator was proposed to sample the received signal at a rate of up to 40 GSPS with a toggle rate of 10 GHz [42].

The proposed UWB computationally-efficient acquisition scheme is distinguished by the fast frequency correlator being used which is the most sizeable operation for DS-UWB baseband signal acquisition. Since its complexity requirements are related to an FFT/IFFT pair and a 1024-points multiplier, then

the total number of the necessary addition and multiplication operations is, respectively approximated as:

$$N_{ADD} = 2M \cdot \log_2 M = 20\ 480\ additions, \quad (17)$$

and

$$N_{MUL} = 2M \cdot \log_2 M + M = 21\ 504\ multiplications. \quad (18)$$

The recent *Virtex* generations of *Xilinx* FPGAs are considered in this paper for the design complexity evaluation. Note that arithmetic functions can be performed through the fast carry logic available on the slices, respectively, in 4 and 2 bits per slice for Virtex-5 and its previous generations (i.e., Virtex-II Pro/Virtex-4) [43], [44]. However, since a 5-bit result is obtained for a 4-bit addition if a carry is allowed, the corresponding cost in terms of slices on Virtex-II Pro/Virtex-4 and Virtex-5, is respectively, the following:

$$\frac{1\ slice \times 5\ bits}{2\ bits} = 2.5\ slices, \quad (19)$$

$$\frac{1\ slice \times 5\ bits}{4\ bits} = 1.25\ slices. \quad (20)$$

Similarly, the 8-bit result obtained by a 4-bit multiplication, corresponds to the following:

$$\frac{1\ slice \times 8\ bits}{2\ bits} = 4\ slices, \quad (21)$$

$$\frac{1\ slice \times 8\ bits}{4\ bits} = 2\ slices. \quad (22)$$

Thus, the total complexity in terms of slices with respect to the used FPGA generation and sampling resolution is presented in Table II.

Notice that only 6 kilobits (i.e., 1 kilobits per user) are needed in terms of RAM resources in the used FPGA to memorize the pre-calculated replicas. If we consider for a single-bit sampling quantization the *XC4VFX140* Virtex-4 chip [45], the UWB fast correlator requires then for its implementation less than 67 % and 0.061 % of slices and RAM resources, respectively. This complexity in terms of slices can be further reduced when considering the two embedded IBM *PowerPC* processors available on this chip. Thus, smaller chips could be used for more compact and optimized complexity.

For a 4-bit sampling quantization, an FPGA-based platform (e.g., based on two FPGAs) appears more appropriate by far for implementing the proposed UWB system. Furthermore, the efficient utilization of the available resources on these chips, such as the *DSP slices* and *PowerPC*, will certainly further optimize the implementation and reduce its cost. If we consider for instance, the Virtex-5 *XC5VLX330T* chip that offers a maximum number of slices of 51,840 and a 11,664 kilobits of RAM resources, an optimal implementation of the studied scheme should make use first of the offered 192 super DSP48E slices before using a second FPGA circuit. Moreover, FPGA-optimized *RF-Engines* cores [37] can also be used for FFT/IFFT to easily achieve a compact hardware implementation of the suggested UWB new scheme.

TABLE II
TOTAL COMPLEXITY IN TERMS OF SLICES

Complexity in Slices	4-bit	1-bit
Virtex-II Pro/Virtex-4	13 7216	41 984
Virtex-5	68 608	20 992

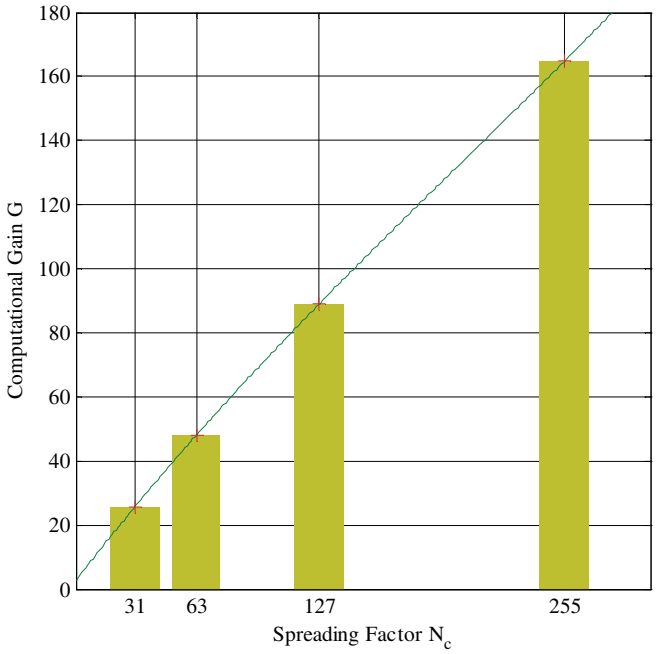

Fig. 6. Gain in complexity with respect to the spreading factor for $N_s = 16$.

D. Gain in Complexity

Assuming that a multiplication computation takes as much as two addition operations, then the total required operations by this UWB acquisition scheme is $6M \log_2 M + 2M$. Thus, the obtained gain in complexity of this proposed fast DS-UWB acquisition system (in comparison to a traditional system that requires M^2 multiplications and $M^2 - 1$ addition operations.) can be illustrated as shown in Fig. 6.

Accordingly, the obtained gain in complexity can be modeled in terms of the used spreading factor as

$$G = 1.5 \cdot 10^{-6} \cdot N_c^3 - 9.2 \cdot 10^{-4} \cdot N_c + 0.77 \cdot N_c + 2.6. \quad (23)$$

We note for a spreading factor of 63, a significant reduction in the computational cost by a factor of about 48. Consequently, the acquisition time is considerably improved with a computational cost reduction.

IV. SIMULATION RESULTS

In this section, the performance of the UWB multiple-access, fast acquisition system in the considered indoor LOS multipath channel scenario is evaluated, by extensive Monte-Carlo simulations in Matlab, using 100 000 samples. Since in the simulations we focus on positioning (when locating the receiver with respect to the other static users), the performance is assessed in terms of the obtained positioning error range which corresponds to the synchronization error obtained while estimating the phase-shift τ. Indeed, assuming that the signals

are transmitted at the speed of light, c, the positioning error range can be computed as $|\tau - \widehat{\tau}| \cdot c$ (using the estimated phase-shift $\widehat{\tau}$). Four different acquisition systems are compared, including ours to validate its score in comparison to the other systems. Furthermore, the performance of the first eleven Gaussian derivatives and the doublet waveforms are compared while used within the studied UWB fast acquisition system to determine the most suitable pulse shape to consider in the multipath scenario for that proposed scheme. Moreover, the obtained performance of the studied computationally-efficient system is compared with respect to the unipath case under different levels of MUI and AWGN. Notice that the unipath case is considered only for comparison purposes. The PN sequences of the acquired user and of the interfering sources are randomly selected for each Monte-Carlo iteration (regardless of any threshold value D_T) from $N_{umax} = 6$ MLS codes of period $N_c = 63$. Moreover, the users are supposed asynchronously in motion inside the mine gallery. Thus, the corresponding phase-shifts are randomly varying within the frame of code-period duration.

Fig. 7 illustrates the performance comparison of the standard acquisition system based on time-domain correlation and the fast acquisition system simulated without an over-sampling method (non-optimal FFT of 1008 points), with *zero-padding*, and finally with the suggested *cubic spline interpolation*. We notice notable performance degradation for the fast acquisition system based on zero-padding. Indeed, this technique changes the circular correlation properties. This is due to the fact that the insertion of the zeros divides the MLS code into two subsequences. Thus, the resulting autocorrelation function contains two neighboring peaks instead of one. Thus, the obtained positioning error range fluctuates, as noticed, slightly with respect to the strongest peak detected between the two neighboring peaks in the resulting autocorrelation function. Fig. 8 shows the obtained autocorrelation function of a zero-padded pulse train showing the two neighboring peaks around the phase-shift of 60 ns. This observed energy loss affects the estimation accuracy and the overall detection capabilities, thus increasing the probability of misdetection.

However, we note for the proposed fast acquisition scheme, based on *interpolation* as an *over-sampling method*, very interesting ranging capabilities with higher levels of accuracy in terms of location estimation in the considered multipath scenario, while also offering an improved acquisition time with a greatly reduced complexity. Indeed, due to the use of higher amount of samples per block (1024 instead of 1008) giving to the handled blocks a higher energy for peak detection, this technique promises the best performance score for the fast acquisition system, in comparison to the other systems.

As noticed, the cubic spline interpolation used as an over-sampling technique changes the overall correlation properties of the pulse shapes. Hence, these will behave herein differently in comparison to other standard acquisition systems. The considered Gaussian-based pulse shapes were run under MUI in extensive Monte-Carlo simulations and compared in the considered multipath context while the noise variance was taken $\sigma_n^2 = 2$. Fig. 9 shows the performance degradation of the simulated waveforms within the proposed fast acquisition system. We notice that the best performance score is obtained

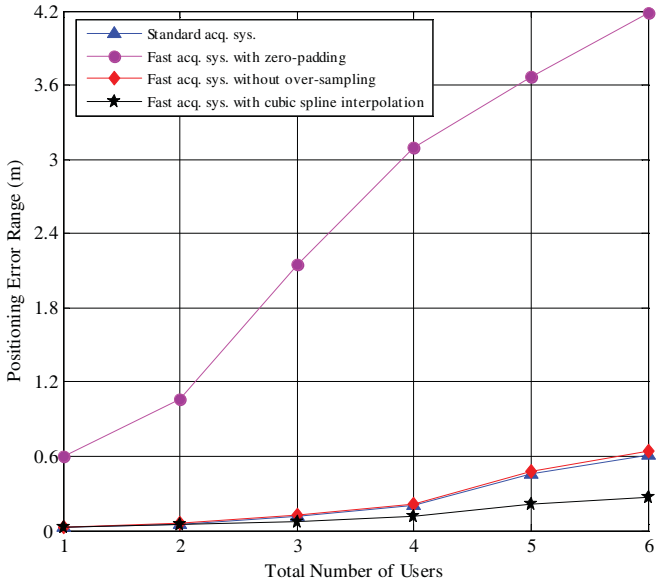

Fig. 7. Performance comparison over a multipath channel under MUI and AWGN ($\sigma_N^2 = 0.5$).

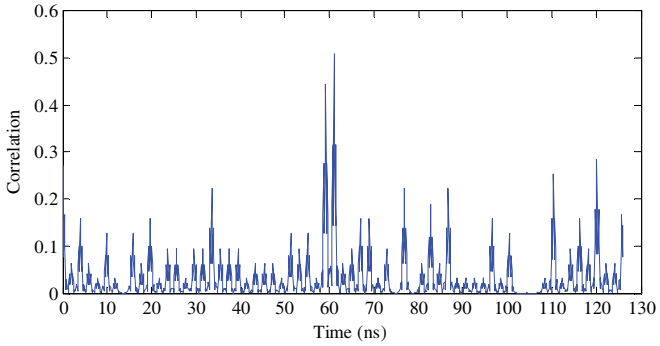

Fig. 8. Autocorrelation function for a zero-padded pulse train.

by the 3^{rd}, 4^{th} and 10^{th} Gaussian derivatives. These waveforms are the most suitable pulse shapes to choose, depending on the spectral bandwidth requirements and compliance to the FCC regulations. Indeed, as the derivative order increases, the peak transmission frequency increases and the signal bandwidth decreases. Hence, choosing the most appropriate derivative order is a trade-off with the pulse shape factor for a desired performance level. Furthermore, it was noticed for the three first Gaussian derivatives, irrespective of their performance, that these pulses do not meet the FCC spectral masks and cannot satisfy it, irrespective of the pulse duration [18]. Therefore, the 4^{th}-order Gaussian derivative has been validated for this studied UWB fast acquisition system in the considered asynchronous multiple-access indoor channel, for simultaneously fulfilling the FCC regulated masks and offering interesting ranging capabilities while maximizing the corresponding bandwidth.

Fig. 10 shows the performance levels for both scenarios of multipath and unipath, compared under different MUI and AWGN levels. From these results, we note a maximum gap of less than 0.6 meters in the positioning error range between the multipath and unipath scenarios. However, since we obtain for the worst case (i.e., maximum interfering sources

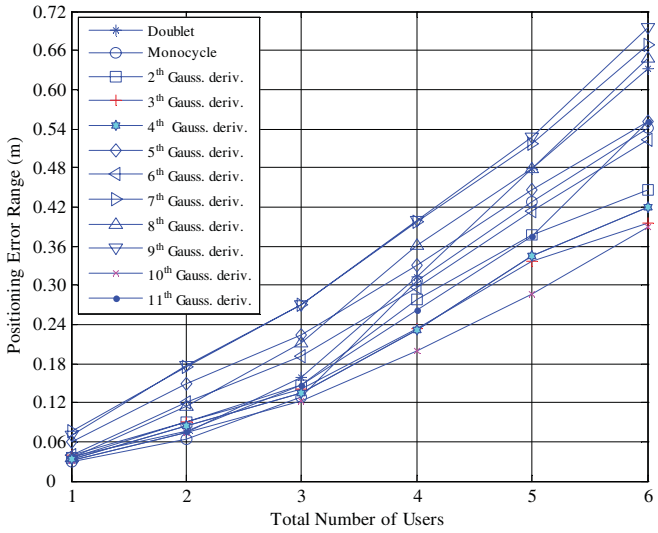

Fig. 9. Pulse shapes performance comparison in multipath scenario under MUI and AWGN ($\sigma_N^2 = 0.5$).

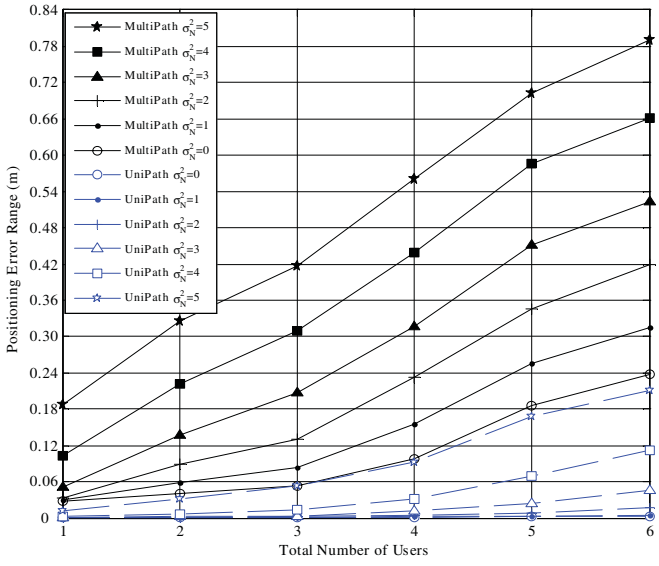

Fig. 10. Performance comparison between multipath and unipath scenarios under MUI and AWGN levels.

within the system with a high level of noise, ($\sigma_N^2 = 5$) a location estimation precision of 0.78 meters which is very acceptable for the desired positioning application, we consider the suggested fast acquisition system well-suited for such underground confined environments.

V. Conclusion

In this paper, an UWB fast acquisition system has been proposed for LOS ranging in an indoor environment. The performance of the suggested computationally-efficient fast acquisition system was assessed and compared in a peculiar indoor multipath fading channel. Simulation results have shown that the proposed fast acquisition scheme based on interpolation offers greatly reduced complexity and acquisition time, while also yielding very promising ranging capabilities at high levels of MUI and AWGN. Furthermore, different Gaussian-based pulses were compared in extensive Monte-Carlo simulations to evaluate their effect on the performance of the suggested system. The results have validated the 4^{th}-order Gaussian derivative as the most suitable pulse shape to adopt for this system operating in such considered confined environment and asynchronous multiple-access scheme. Moreover, comparisons of the suggested fast acquisition system have been made between the considered multipath fading channel and a unipath scenario, with respect to the obtained location estimation precision. The proposed system has shown very acceptable positioning error range for the considered indoor LOS environment.

References

[1] M. Z. Win and R. A. Scholtz, "Impulse radio: how it works," *IEEE Commun. Lett.*, vol. 2, no. 2, pp. 36–38, Feb. 1998.

[2] A. Dogandzic, J. Riba, G. Seco, and A. L. Swindlehurst, "Positioning and navigation with applications to communications," *IEEE Signal Process. Mag.*, vol. 22, no. 4, pp. 10–11, July 2005.

[3] Federal Communications Commission, "Revision of part 15 of the commission's rules regarding ultra-wideband transmission systems," First Report and Order, ET Docket 98-153, Apr. 2002.

[4] W. Namgoong, "A channelized digital ultra-wideband receiver," *IEEE Trans. Wireless Commun.*, vol. 2, pp. 502–510, May 2003.

[5] L Reggiani and G. M. Maggio, "On the acquisition time for serial and parallel code search in UWB impulse radio," in *Proc. IEEE Int. Symp. on Circuits & Systems*, vol. 1, pp. 53–56, May 2005.

[6] L Reggiani and G. M. Maggio, "Rapid search algorithms for code acquisition in UWB impulse radio communications," *IEEE J. Sel. Areas Commun.*, vol. 23, no. 5, pp. 898–908, May 2005.

[7] S. R. Aedudodla, S. Vijayakumaran, and T. F. Wong, "Timing acquisition in ultra-wideband communication systems," *IEEE Trans. Veh. Technol.*, vol. 54, no. 5, pp. 1570–1583, Sep. 2005.

[8] W. Suwansantisuk, M. Z. Win, and L. A Shepp, "On the performance of wide-bandwidth signal acquisition in dense multipath channels," *IEEE Trans. Veh. Technol.*, vol. 54, no. 5, pp. 1584–1594, Sep. 2005.

[9] W. Suwansantisuk and M. Z. Win, "Multipath aided rapid acquisition: optimal search strategies," *IEEE Trans. Inf. Theory*, vol. 53, no. 1, pp. 174–193, Jan. 2007.

[10] N. He and C. Tepedelenlioglu, "Fast and low-complexity frame-level synchronization for transmitted reference receivers," *IEEE Trans. Wireless Commun.*, vol. 6, no. 3, pp. 1014–1023, Mar. 2007.

[11] M. Di Renzo *et al.*, "A novel class of algorithms for timing acquisition of differential transmitted reference UWB receivers: architecture, performance analysis and system design," *IEEE Trans. Wireless Commun.*, vol. 7, no. 6, pp. 2368–2387, 2008.

[12] C. Nerguizian, C. Despins, S. Affes, and M. Djadel, "Radio channel characterization of an underground mine at 2.4 GHz," *IEEE Trans. Wireless Commun.*, vol. 4, no. 5, pp. 2441–2453, Sep. 2005.

[13] M. Boutin, A. Benzakour, C. Despins, and S. Affes, "Radio wave characterization and modeling in underground mine tunnels," *IEEE Trans. Antennas Propag.*, vol. 56, no. 2, pp. 540–549, Feb. 2008.

[14] C. Nerguizian, "Radiolocation in an underground mining environment," Ph.D. dissert., INRS-EMT, Montreal, Canada, Sep. 2003.

[15] Y. Salih Alj, C. Despins, and S. Affes, "A computationally efficient implementation of a UWB fast acquisition scheme," in *Proc. IEEE VTC'07-Spring*, pp. 1554–1558, Apr. 2007.

[16] M. Welborn and J. McCorkle, "The importance of fractional bandwidth in ultra-wideband pulse design," in *Proc. IEEE Int. Conf. Communications*, vol. 2, pp. 753–757, Apr. 2002.

[17] H. Sheng, P. Orlik, A. M. Haimovich, L. J. Cimini, and J. Zhang, "On the spectral and power requirements for ultra-wideband transmission," in *Proc. IEEE Int. Conf. Communications*, vol. 1, pp. 738–742, May 2003.

[18] B. Hu and N. C. Beaulieu, "Pulse shapes for ultrawideband communication systems," *IEEE Trans. Wireless Commun.*, vol. 4, no. 4, pp. 1789–1797, July 2005.

[19] M. U. Mahfuz, K. M. Ahmed, R. Ghimire, and R. M. A. P. Rajatheva, "Performance comparison of pulse shapes in STDL and IEEE 802.15.3a models of the UWB channel," in *Proc. IEEE ICICS'05*, pp. 811–815, Dec. 2005.

[20] V. S. Somayazulu, J. R. Foerster, and S. Roy, "Design challenges for very high data rate UWB systems," in *Proc. 36th Asilomar Conference on Signals, Systems and Computers*, vol. 1, pp. 717–721, Nov. 2002.

[21] J. R. Foerster, M. Pendergrass, and A. F. Molisch, "A channel model for ultrawideband indoor communication," in *Proc. Wireless Personal Multimedia Communications*, vol. 2, pp. 116–120 Oct. 2003.
[22] Y. Rissafi, "Characterization and modeling of ulta-wideband channel in an underground mine," Masters's thesis, University of Quebec at Outaouais, Canada, June 2007.
[23] A. A. Saleh and R. A. Valenzuela, "A statistical model for indoor multipath propagation," *IEEE J. Sel. Areas Commun.*, vol. 5, no. 2, pp. 128–137, Feb. 1987.
[24] A. F. Molisch *et al.*, "A comprehensive standardized model for ultrawideband propagation channels," *IEEE Trans. Antennas Propag.*, vol. 54, no. 11, pp. 3151–3166, Nov. 2006.
[25] Z. N. Low *et al.*, "Pulse detection algorithm for line-of-sight (LOS) UWB ranging applications," *IEEE Antennas Wireless Propag. Lett.*, vol. 4, pp. 63–67, 2005.
[26] D. Cassioli, M. Z. Win, and A. F. Molisch, "The ultra-wide bandwidth indoor channel: from statistical model to simulations," *IEEE J. Sel. Areas Commun.*, vol. 20, no. 6, pp. 1247–1257, Aug. 2002.
[27] M. Hamalainen *et al.*, "Wideband radio channel measurement in a mine," in *Proc. 5th Int. Symp. on Spread Spectrum Techniques and Applications*, vol. 2, pp. 522–526, Sep. 1998.
[28] S. A. Fares, *et al.*, "Efficient sequential blind beamforming for wireless underground communications," in *Proc. IEEE VTC'06-Fall*, pp. 1–4, Sep. 2006.
[29] S. A. Fares, *et al.*, "Fractional-delay sequential blind beamforming for wireless multipath communications in confined areas," *IEEE Trans. Wireless Commun.*, vol. 7, no. 2, pp. 629–638, Feb. 2008.
[30] C. J. Alpert, *et al.*, "Delay and slew metrics using the lognormal distribution," in *Proc. Design Automation Conf.*, pp. 382–385. 2003.
[31] J. G. Ackenhusen, *Real-Time Signal Processing: Design and Implementation of Signal Processing Systems*. Prentice Hall, 1999.
[32] P. M. Gerard, G. P. M. Egelmeers, and P. C. W. Sommen, "A new method for efficient convolution in frequency domain by nonuniform partitioning for adaptive filtering," *IEEE Trans. Signal Process.*, vol. 44, no. 12, pp. 3123–3129, Dec. 1996.
[33] D. J. R. Van Nee and A. J. R. M. Coenen, "New fast GPS code-acquisition technique using FFT," *IEEE Electron. Lett.*, vol. 27, pp. 158–160, Jan. 1991.
[34] R. A. Stirling-Gallacher, A. P. Hulbert, and G. J. R. Povey, "A fast acquisition technique for a direct sequence spread spectrum signal in the presence of a large Doppler shift Spread," in *Proc. IEEE 4th Inter. Symp. on Spectrum Tech. & App.*, vol. 1, pp. 156–160, 1996.
[35] G. Feng and F. Van Graas, "GPS receiver block processing," in *Proc. ION Instit. of Navigation GPS'99*, pp. 307-316, Sep. 1999.
[36] O. A. Mukhanov *et al.*, "High-resolution ADC operation up to 19.6 GHz clock frequency," *IoP J. Superconductor Science and Technol.*, pp. 1065–1070, Nov. 2001.
[37] URL: http://www.rfel.com/download/D04026_FFT_Product_Sheet.pdf
[38] D. Wentzloff *et al.*, "System design considerations for ultra-wideband communications," *IEEE Commun. Mag.*, vol. 43, no. 8, pp. 114–121, Aug. 2005.
[39] J. Nielsen and R. Pasand, "Ultra-wideband rake receiver based on single-bit processing," in *Proc. IEEE Can. J. Elect. Comput. Eng.*, vol. 31, no.1, Winter 2006.
[40] W. Ellersick *et al.*, "GAD: a 12-GS/s CMOS 4-bit A/D converter for an equalized multi-level link," in *Proc. Symp. VLSI Circuits*, pp. 49–52, June 1999.
[41] X. Zhang and M. Bayoumi, "A low power 4-bit interleaved burst sampling ADC for sub-GHz impulse UWB radio," in *Proc. IEEE ISCAS'2007*, pp. 1165–1168, May 2007.
[42] Y. Okaniwa *et al.*, "A 40-Gb/s CMOS clocked comparator with bandwidth modulation technique," *IEEE J. Solid-State Circuits*, vol. 40, no.8, pp. 1680–1687, Aug. 2005.
[43] E. Garcia, "Desinging properly with FPGAs," *MVD Company Electronic Publications*, no. 125, pp. 2–6, May 2002. URL: http://www.mvd-fpga.com/fr/publications.html
[44] URL: http://www.xilinx.com/support/documentation/data_sheets/ds100.pdf Xilinx, "Virtex-5 Family Overview LX, LXT, and SXT Platforms," Feb. 2007.
[45] URL: http://www.xilinx.com/support/documentation/data_sheets/ds112.pdf Xilinx, "VVirtex-4 Family Overview LX, SX, and FX Platforms," Sep. 2007.

Yassine Salih-Alj (S'08-M'10) received the Bachelor's degree in microelectronics from the University of Quebec at Montreal (UQAM), Montreal, Quebec, Canada, in 2001, and the Master's degree in electrical engineering from the École de Technologie Supérieure (ETS), Montreal, Quebec, Canada, in 2003, and the Ph.D. degree in Telecommunications from the National Institute of Scientific Research - Energy, Materials & Telecommunications (INRS-Telecom), Montreal, Quebec, Canada, in 2008. He served as a research assistant at the Telebec Underground Communications Research Laboratory (LRTCS) from 2005 to 2008, and then during 2009 as a Postdoctoral Fellow at Poly-Grames Research Center, of the École Polytechnique de Montréal, Montreal, Quebec, Canada. He is currently working as a permanent faculty member at the School of Science and Engineering (SSE) of Al Akhawayn University in Ifrane (AUI), Morrocco.

Charles Despins (S'93-M'94-SM'02)' career has spanned both the academic and industry segments of the information and communications technologies (ICT). In addition to his work as a faculty member of INRS-Telecommunications (Université du Québec) in Montreal, Canada, he has held various posts in the private sector, namely at CAE Electronics, Microcell Telecommunications (Canadian cellular operator) and at Bell Nordiq Group (a network operator in rural and northern areas of Canada) as vice-president and chief technology officer. He has also worked as a consultant for wireless network deployments in India and China. Since January 2003, he has been president and CEO of Prompt inc., an ICT university-industry research and development consortium. In addition, he is an adjunct professor at INRS-EMT (Université du Québec) and a faculty member (on leave) at École de Technologie Supérieure (Université du Québec) in Montreal, with research interests in wireless communications. He is also a guest lecturer in the executive MBA program at McGill University in Montreal.

He holds a bachelors degree in electrical engineering from McGill University in Montreal, Canada as well as M.Sc. and Ph.D. degrees, also in electrical engineering, from Carleton University in Ottawa, Canada. Dr. Despins is a past recipient (1993) of the Best-Paper-of-the-Year award in IEEE TRANSACTIONS ON VEHICULAR TECHNOLOGY and he was General co-Chair of the 2006-Fall IEEE Vehicular Technology Conference. He is also a Fellow (2005) of the Engineering Institute of Canada and a recipient (2006) of the Outstanding Engineer award from IEEE Canada.

Sofiène Affes (S'94-M'95-SM'04) received the Diplôme d'Ingénieur in electrical engineering in 1992, and the Ph.D. degree with honors in signal processing in 1995, both from the École Nationale Supérieure des Télécommunications (ENST), Paris, France. He has been since with INRS-EMT, University of Quebec, Montreal, Canada, as a Research Associate from 1995 till 1997, as an Assistant Professor till 2000, then as an Associate Professor till 2009. Currently he is a Full Professor in the Wireless Communications Group. His research interests are in wireless communications, statistical signal and array processing, adaptive space-time processing. From 1998 to 2002 he has been leading the radio-design and signal processing activities of the Bell/Nortel/NSERC Industrial Research Chair in Personal Communications at INRS-EMT, Montreal, Canada. Since 2004, he has been actively involved in major projects in wireless of PROMPT (Partnerships for Research on Microelectronics, Photonics and Telecommunications).

Professor Affes was the co-recipient of the 2002 Prize for Research Excellence of INRS. He currently holds a Canada Research Chair in Wireless Communications and a Discovery Accelerator Supplement Award from NSERC (Natural Sciences & Engineering Research Council of Canada). In 2006, Professor Affes served as a General Co-Chair of the IEEE VTC2006-Fall conference, Montreal, Canada. In 2008, he received from the IEEE Vehicular Technology Society the IEEE VTC Chair Recognition Award for exemplary contributions to the success of IEEE VTC. He currently acts as a member of the Editorial Boards of the IEEE TRANSACTIONS ON WIRELESS COMMUNICATIONS, THE IEEE TRANSACTIONS ON SIGNAL PROCESSING, and the *Wiley Journal on Wireless Communications & Mobile Computing*.